Soft Computing (2024) 28:7125–7137
https://doi.org/10.1007/s00500-023-09600-z

OPTIMIZATION

A multi-UAV assisted non-orthogonal multiple access based relay system for minimal average receiving rate maximization

Qiang Tang[1,2] · Xinyu Qu[1,2] · Jin Wang[1,2] · Shiming He[1,2]

Accepted: 15 December 2023 / Published online: 26 January 2024

Abstract

In this paper, we proposed a data relay system consisting of multiple unmanned aerial vehicles (UAVs) and acess point (AP) with the aim of maximizing the minimum receiving rate of Internet of things devices (IoTDs) as the optimization objective. To enhance the utilization of communication resources, we employed non-orthogonal multiple access (NOMA) and successive interference cancellation (SIC) techniques at the AP side. In addition, we used the Wireless power transmission (WPT) technique on the UAV side to charge the IoTDs and prolong their operational lifetime. We formulated the problem as a mixed integer nonlinear programming (MINLP). To solve the MINLP problem, it was decomposed into four subproblems: connection scheduling between UAVs and IoTDs, time slot allocation, UAV trajectory, and AP's power distribution. Finally, we solved all subproblems by using convex optimization techniques, such as successive convex approximations (SCA), and proposed an iterative algorithm. In the simulation, we compared our proposed algorithm with different optimization schemes. The results indicated that our scheme outperforms the others.

Keywords Data relay system · Non-orthogonal multiple assess · UAV trajectory optimization · Mimimal average receiving rate maximization

1 Introduction

Thanks to their high mobility and flexibility, UAVs can serve as Mobile Edge Computing (MEC) platforms for processing data offloaded by IoTDs (Seid 2021; Wang 2018b; Liu et al. 2022). Additionally, they can act as relay devices to transmit tasks to base stations for computation (Baek and Lim 2019; Zhong et al. 2019). Although traditional fixed relay devices have been extensively studied, it is difficult to meet the communication needs in complex terrain environments (Jing and Jafarkhani 2009; Kim et al. 2015; Gao et al. 2019). Compared to traditional fixed relay devices, UAVs possess the unique capability to adjust their positions based on device locations. This feature is particularly advantageous for delay-sensitive tasks as it enables us to determine the optimal position of UAVs to meet low-delay requirements. Furthermore, UAVs, being aerial platforms, excel at navigating complex terrains. Unlike traditional relay devices that are easily obstructed, UAVs flying at high altitudes can establish Line-of-Sight (LoS) communication with devices (You and Zhang 2020). UAVs can also act as relay devices to forward data from base stations to IoTDs in certain scenarios, such as post-disaster relief. After the base stations in the disaster area are destroyed, the trapped people are unable to receive information from the outside world. Therefore, we can deploy UAVs as temporary communication devices to relay external information and safety instructions to portable communication devices, such as smartphones and smartwatches, carried by the trapped individuals.

✉ Qiang Tang
tangqiang@csust.edu.cn

Xinyu Qu
21208051610@stu.csust.edu.cn

Jin Wang
jinwang@csust.edu.cn

Shiming He
smhe_cs@csust.edu.cn

[1] School of Computer Science and Communication Engineering, Changsha University of Science and Technology, Changsha, Hunan, China

[2] Hunan Provincial Key Laboratory of Intelligent Processing of Big Data on Transportation, School of Computer and Communication Engineering, Changsha University of Science and Technology, Changsha 410004, People's Republic of China

In this paper, we proposed a relay system consisting of multiple UAVs and an AP, where the AP is responsible for sending data to the UAVs and the UAVs are responsible for forwarding the data from the AP to IoTDs. To ensure reliable data delivery, we employ the Wireless Power Transmission (WPT) technique, enabling UAVs to charge the IoTDs. Finally, we have maximized the average minimum rate at which IoTDs receive data as the optimization objective. The main contributions are as follows:

(1) The NOMA and SIC techniques are used to enhance the communication rate between the AP and UAVs. Additionally, we proposed a parameter optimization problem based on power allocation for the AP. The problem strictly follows the SIC demodulation order. Since this problem is a non-convex problem, we solved it using convex optimization methods such as SCA and obtained an approximate optimal solution for power allocation.
(2) To further solve the problem of time slot allocation problem. We divided the entire cycle into multiple sub-slots. Each sub-slots is used for data transmission between the AP and UAV, power transmission between the UAV and IoTDs, and data transmission between the UAV and IoTDs, respectively. Since the problem is a linear programming problem, it was solved by CVX solver.
(3) Since multi-UAV trajectory optimization is a nonconvex problem with complex mixed variables, we optimized the trajectory of each UAV step by step while fixing the trajectories of other UAVs by the BCD method. The nonconvex constraint was transformed by introducing relaxation variables and using the SCA technique to obtain an approximate optimal solution for the trajectory.
(4) In the simulation results, we not only demonstrated the performance of the algorithm against other optimization methods, but also compared the difference in UAV receiving rate between OFDMA and NOMA schemes. Finally, we also investigated the effect of different parameters such as maximum flight speed, system period, UAV flight altitude, and UAV transmitting power, on the optimization objective.

2 Related work

2.1 UAV-assisted relay system

In the papers (Li et al. 2019; Wang 2018a), the authors discussed the latest advancements and future prospects of UAV communication in the 5 G era and beyond. In Li et al. (2019), the authors discussed the capabilities of UAVs. They highlighted that UAVs can not only perform data forwarding but also transmit energy to users using WPT technology. Furthermore, the authors mentioned that the flight time of UAVs can be extended by equipping them with solar panels to collect energy. In Zeng et al. (2016), Zeng et al. proposed a UAV-supported relay model. The communication from source to destination nodes was achieved by deploying UAVs as relay systems. The transmitting power of the source node and relay, and flight trajectory of the UAV were optimized to maximize the throughput of the system. Ji et al. in Ji (2020) considered the deployment of a UAV relay in the case of difficult communication between the base station and user. The sum of transmission rates of all users was maximized by optimizing the UAV trajectory, speed, acceleration, and scheduling of UAVs and devices. In Liu (2023), Liu et al. considered the worst-case scenario of car and base station communication, taking into account the presence of eavesdroppers. They proposed the deployment of UAVs with reconfigurable smart surfaces as relay systems to assist communication. In Jiang et al. (2019), Jiang et al. designed a UAV-assisted relay system to forward data from multiple ground devices via time division multiple access. The authors optimized the time slot allocation, power allocation, and UAV flight trajectory to maximize the minimum average data rate of each communication pair. In Zhang (2022), Zhang et al. proposed a multi-UAV collaborative relay system to enhance the duration of communication. Specifically, multiple UAVs work one after the other as substitutes. The authors designed heuristic substitution and spectrum effect substitution schemes.

2.2 UAV-assisted NOMA technology

In recent years, there has been extensive research on Non-Orthogonal Multiple Access (NOMA) technology (Yadav et al. 2020; Zeng 2018; Liu et al. 2019). NOMA has garnered significant attention due to its potential for improving spectral efficiency and accommodating a large number of users in wireless communication systems. Due to the limited frequency band resources, many studies on MEC considered the application of NOMA technology. In Diao et al. (2019), Diao et al. proposed a UAV-assisted mobile edge computing system based on NOMA technology to minimize the maximum energy consumption among all users by optimizing trajectories, task data, and computational resource allocation. Katwe et al. in Katwe et al. (2021) designed an unconventional two-stage dynamic user interface. Clustering user nodes to reduce interference between multiple UAVs. In the first step, all user nodes will be divided into groups equal to the number of UAVs using the k-means algorithm. Then, the user nodes are further divided into dynamic number of sub-clusters using elbow method, and k-means method based on their distribution location. Rezvani et al. in Rezvani et al. (2022) proposed globally optimal power allocation strategies to maximize the total rate and energy efficiency as the optimization objectives,

respectively, and solved them by the fast water-filling algorithm and the Dinkelbach algorithm. Wang (2020a) proposed a device-to-device-enhanced UAV-NOMA network architecture that allowed ground users who have already received File Blocks (FBs) to reuse the time–frequency resources assigned to NOMA links to share their FBs with other ground users. In Mirbolouk et al. (2022), authors deployed UAVs to act as relay systems for satellites and ground equipment and proposed a hybrid satellite-unmanned aerial vehicle (UAV) relay network (HSURN). Meanwhile, the authors used coordinated multi-point transmission and NOMA techniques to enhance the spectral efficiency.

The work in Ji (2020) and Mirbolouk et al. (2022) are the most relevant with our research work. However, the authors in Ji (2020) did not consider the deployment of multiple UAVs, and the optimization target was the sum of transmission rates for all users. This approach results in low transmission rates for certain users. The work in Mirbolouk et al. (2022) did not apply the WPT technology and did not consider the AP and UAV communication processes in the model. In this paper, we proposed a system that combined a single AP and multi-UAV. The spectrum efficiency was enhanced by using NOMA and SIC techniques during the process of transmitting data from AP to UAVs. In addition we have targeted to maximize the minimum average receiving rate among the IoTDs. Finally, the simulation results showed that our model was superior to other.

The rest of the paper is organized as follows, Sect. 3. introduces our system model and Problem Formulation, and Sect. 4 describes the problem solving process. In Sect. 5, we presented the simulation results and analyze the data. Finally, we concluded the paper in Sect. 6.

3 System model and problem formulation

3.1 System model

Our system includes U rotary wing UAVs, K IoTDs and one AP. As shown in Fig. 1, the workflow of the entire system is as follows: The AP initially sends data to the UAVs, which receive the data and then transmit power to the connected IoTDs before forwarding the data. The UAV receives and forwards the data in frequency-division duplexing (FDD) mode. The horizontal coordinates of the kth IoTD correspond to $w_k = [x_k, y_k]^T$, where $k \in \mathcal{K} = \{1, 2,..., K\}$, and the ground coordinates of the AP are $w_m = [x_m, y_m]^T$. For quantitative analysis, the entire flight period T of the UAV is divided equally into N time slots. Each time slot has a length of t, calculated as T/N. The value of N is large enough to ensure that the UAV is considered immobile in each time slot. The flight altitude of all UAVs is denoted as H, and the horizontal coordinates of the $u \in \mathcal{U}=\{1,2,...,U\}$ UAV at the n-th $\in \mathcal{N}=\{1,2,...,N\}$ time slot is $q_u[n]=[x_u[n],y_u[n]]^T$.

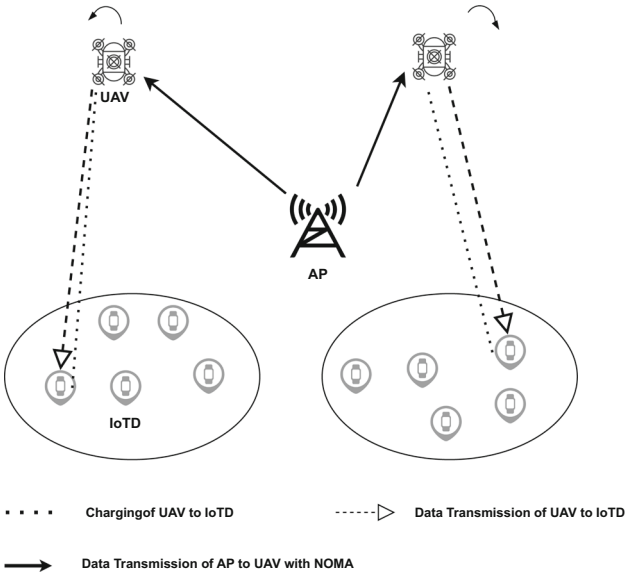

Fig. 1 The system model

Notably, we assumed that UAVs fly according to a periodic pattern, so that the initial position $q_u[1]$ and final position $q_u[N]$ of the u-th UAV are equal.

$$q_u[1] = q_u[N] \quad \forall u \in \mathcal{U} \tag{1}$$

The maximum flight speed of the UAV is set to V_{max}, and to prevent collisions of UAVs, we set a safe distance d_{min} to ensure that no collisions occur between UAVs, in which all UAVs should satisfy both speed and anti-collision constraints.

$$\| q_u[n+1] - q_u[n] \|^2 \le (V_{\max} t)^2 \quad \forall u \in \mathcal{U}, n \in \mathcal{N} \tag{2}$$

$$\| q_j[n] - q_k[n] \|^2 \ge (d_{\min})^2 \quad \forall j, k \in \mathcal{U}\ j \ne k \tag{3}$$

To simplify the analysis, we made an assumption regarding the area of operation for the multiple unmanned systems. We assumed that the area is an open space, where the influence of terrain and obstacles can be disregarded. Additionally, we assumed that there is no occlusion from UAVs to IoTDs and AP. Therefore, our data transmission can be considered as LoS transport. The channel gains from the UAV to the AP and the IoTD are denoted as $h_{au}[n]$ and $h_{uk}[n]$, respectively. The relevant channel formula is as follows.

$$h_{au}[n] = \beta_0 d_{au}^{-2}[n] \tag{4}$$

$$h_{uk}[n] = \beta_0 d_{uk}^{-2}[n] \tag{5}$$

where β_0 indicates the channel power gain at the unit distance d_0 =1 m. d_{au} and d_{uk} represent the distance from the u-th

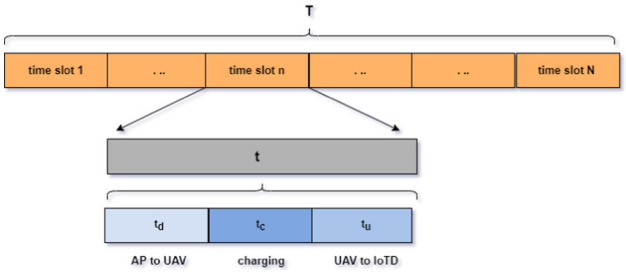

Fig. 2 The communication model

UAV to the AP and the k-th IoTD respectively, which can be expressed as

$$d_{au}[n] = \sqrt{H^2 + \| q_u[n] - w_m \|^2} \tag{6}$$

$$d_{uk}[n] = \sqrt{H^2 + \| q_u[n] - w_k \|^2} \tag{7}$$

We defined $a_{uk}[n]$ as the connection scheduling between the u-th UAV and the k-th IoTD at the n-th time slot. $a_{uk}[n]$=1 indicates that the u-th UAV and k-th IoTD establish a connection at the n-th time slot. 0 means no connection.

$$\sum_{k=1}^{K} a_{uk}[n] = 1 \quad \forall n \in \mathcal{N}, u \in \mathcal{U} \tag{8}$$

$$\sum_{u=1}^{U} a_{uk}[n] = 1 \quad \forall n \in \mathcal{N}, \forall k \in \mathcal{K} \tag{9}$$

$$a_{uk}[n] \in \{0, 1\} \quad \forall k \in \mathcal{K}, u \in \mathcal{U}, n \in \mathcal{N} \tag{10}$$

Constraint (8) indicates that one UAV can only connect to one IoTD at each time slot, and equation (9) means that a UAV can be only connected to one IoTD per time slot.

The communication model of the entire system is shown in Fig. 2. We divided each time slot into three subslots: the transmission time $t_d[n]$ from the AP to UAVs, the transmission time $t_u[n]$ from UAVs to IoTDs, and the time $t_c[n]$ for power transmission from UAVs to IoTDs. It was worth noting that AP can send data to multi-UAV at the same time, but UAVs can only send data to one IoTD in single time slot. The relevant constraint can be expressed as follows.

$$0 \le t_d[n] \le t \quad \forall n \in \mathcal{N} \tag{11}$$

$$0 \le t_u[n] \le t \quad \forall n \in \mathcal{N} \tag{12}$$

$$0 \le t_c[n] \le t \quad \forall n \in \mathcal{N} \tag{13}$$

$$t_d[n] + t_u[n] + t_c[n] = t \quad \forall n \in \mathcal{N} \tag{14}$$

Based on the rules of NOMA in the downlink capacity domain. The NOMA transmitter sends the data of different users overlapping each other, while the receiver distinguishes between the signals of different users based on their respective signal strengths. Therefore, the power level assigned to different users at the transmitter side directly affects the demodulation performance of the SIC receiver and also determines the sum rate of the NOMA system (Islam et al. 2016; Miridakis and Vergados 2012). In our system, we allocated more power to the UAV with a weaker channel gain to ensure the basic data rate requirement. It is assumed that the channel gain satisfies $h_{a1} < h_{a2} \ldots < h_{au} < \cdots h_{mU}$, then the transmitted power have $P_1 > P_2 \cdots > P_u > \ldots P_U$.

During the data transmission from the AP to UAVs, the amount of data sent by the AP to the u-th UAV in the n-th time slot is

$$D_{au}[n] = B_u \log_2 \left(1 + \frac{P_u[n] h_{au}[n]}{\delta^2 + \sum_{j=u+1}^{U} P_j[n] h_{aj}[n]} \right) t_d[n] \tag{15}$$

where B_u, δ^2 and $P_u[n]$ are the Bandwidth between AP and UAV, noise power and transmitting power from the AP to the u-th UAV, respectively.

From Eq. (15), we can see that we should prioritize demodulating the UAV with the worst channel gain and then remove it from the superimposed signals. Because its assigned power is the largest, it causes more interference to other UAVs. At this point, we considered the signals from other UAVs to be interfering with our signals. Then, the UAV with the second lowest channel gain is demodulated and removed from the superimposed signal. This process is repeated until all UAVs' data has been demodulated.

The total transmit power of the AP is P_{ap}. The sum of the power allocated by the AP to the UAVs in each time slot should be equal to its total power, and the power allocated to each UAV should not exceed its total power.

$$\sum_{u=1}^{U} P_u[n] \le P_{ap} \quad \forall n \in \mathcal{N} \tag{16}$$

$$0 \le P_u[n] \le P_{ap} \quad \forall n \in N, u \in \mathcal{U} \tag{17}$$

The size of the data volume sent by the u-th UAV to the k-th IoTD in the n-th time slot is

$$D_{uk}[n] = \log_2 \left(1 + \frac{P_{uav} h_{uk}[n]}{\delta^2 + \sum_{j=1, j \ne u}^{U} P_{uav} h_{jk}[n]} \right) \times a_{uk}[n] B_i t_u[n] \tag{18}$$

where, P_{uav} indicates the transmitting power of the UAV. B_i is the bandwidth between the UAV and the IoTD.

Meanwhile, the amount of data forwarded by the UAV to the IoTD at each time slot cannot exceed the amount received from the AP at that same time slot.

$$D_{au}[n] \geq D_{uk}[n] \quad n \in \mathcal{N} \tag{19}$$

The average receiving rate of IoTD k during the entire duty cycle is the total data volume divided by the total time.

$$R_k = \frac{1}{Nt} \sum_{u=1}^{U} \sum_{n=1}^{N} D_{uk}[n] \tag{20}$$

We assumed that a UAV charges IoTD with a constant power P_c before transmiting data to the connect IoTD. So the energy collected by the IoTD during the n-th slot can be written as

$$E_k[n] = \varepsilon P_c a_{uk}[n] h_{uk}[n] t_c[n] \tag{21}$$

where ε indicates the energy conversion efficiency, which is restricted to (0, 1]. To ensure that IoTDs have enough power to receive data transmitted from UAVs. We required that the energy received by the IoTD at this time slot is greater than the energy consumed by it to receive the data.

$$E_k[n] \geq a_{uk}[n] P_{iotd} t_u[n] \quad \forall k \in \mathcal{K}, n \in \mathcal{N}, u \in \mathcal{U} \tag{22}$$

where P_{iotd} is the power of IoTDs when receiving data.

3.2 Problem formulation

Our optimization variables are connection scheduling $\boldsymbol{A} = \{a_{uk}[n],\ \forall k \in \mathcal{K}, u \in \mathcal{U}, n \in \mathcal{N}\}$, UAV's data receiving rate time $\boldsymbol{t_u} = \{t_u[n],\ n \in \mathcal{N}\}$, UAV's data forwarding time $\boldsymbol{t_d} = \{t_d[n],\ n \in \mathcal{N}\}$, UAV's charging time $\boldsymbol{t_c} = \{t_c[n],\ n \in \mathcal{N}\}$, transmitting power of AP $\boldsymbol{P} = \{P_u[n],\ n \in \mathcal{N},\ u \in \mathcal{U}\}$ and UAV's flight trajectory $\boldsymbol{Q} = \{q_u[n],\ n \in \mathcal{N},\ u \in \mathcal{U}\}$. Our object is to maximize the one with the lowest average receiving rate among all IoTDs by optimizing the variables $\boldsymbol{A}$, $\boldsymbol{t_u}$, $\boldsymbol{t_d}$, $\boldsymbol{t_c}$, $\boldsymbol{P}$ and $\boldsymbol{Q}$. For simplicity, we introduced the variable $\mathrm{Z} = \min R_k, k \in \mathcal{K}$. So, the optimization problem can be formulated as

(**P1**) :

$$\max_{A, t_u, t_d, t_c, Q, \mathrm{Z}, \mathrm{P}} \quad \mathrm{Z} \tag{23a}$$

$$s.t. \quad \mathrm{R_k} \geq Z \quad \forall k \in \mathcal{K} \tag{23b}$$

$$E_k[n] \geq a_{uk}[n] P_{iotd} t_u[n] \quad \forall k \in \mathcal{K}, n \in \mathcal{N}, u \in \mathcal{U} \tag{23c}$$

$$D_{au}[n] \geq D_{uk}[n] \quad n \in \mathcal{N}, u \in \mathcal{U}, k \in \mathcal{K} \tag{23d}$$

$$q_u[1] = q_u[n] \quad \forall u \in \mathcal{U} \tag{23e}$$

$$\sum_{k=1}^{K} a_{uk}[n] = 1 \quad \forall n \in \mathcal{N}, u \in \mathcal{U} \tag{23f}$$

$$\sum_{u=1}^{U} a_{uk}[n] = 1 \quad \forall n \in \mathcal{N}, k \in \mathcal{K} \tag{23g}$$

$$a_{uk}[n] \in \{0, 1\} \quad \forall k \in \mathcal{K}, u \in \mathcal{U}, n \in \mathcal{N} \tag{23h}$$

$$0 \leq t_u[n] \leq t, 0 \leq t_d[n] \leq t, 0 \leq t_c[n] \leq t \quad \forall n \in \mathcal{N} \tag{23i}$$

$$t_d[n] + t_u[n] + t_c[n] = t \quad \forall n \in \mathcal{N} \tag{23j}$$

$$\| q_u[n+1] - q_u[n] \|^2 \leq (V_{\max} t)^2 \quad \forall u \in \mathcal{U}, n \in \mathcal{N} \tag{23k}$$

$$\| q_j[n] - q_k[n] \|^2 \geq (d_{\min})^2 \quad \forall j, k \in \mathcal{U}, j \neq k \tag{23l}$$

$$\sum_{u=1}^{U} P_u[n] \leq P_{ap} \quad \forall n \in \mathcal{N} \tag{23m}$$

$$0 \leq P_u[n] \leq P_{ap} \quad \forall n \in N, u \in \mathcal{U} \tag{23n}$$

$$P_{ap} > P_1[n] > P_2[n] ... > P_U[n] \geq 0 \quad \forall n \in \mathcal{N} \tag{23o}$$

(P1) is a MINLP, NP-hard problem, then we will decompose it into some subproblems and use the BCD method to solve them.

4 Problem solving

4.1 Connection scheduling optimization

To optimize $\boldsymbol{A}$ with fixed $\boldsymbol{t_u}$, $\boldsymbol{t_d}$, $\boldsymbol{t_c}$, $\boldsymbol{Q}$ and $\boldsymbol{P}$, the objective function and the related constraints can be written as

(**P2**) :

$$\max_{A, \mathrm{Z}} \quad \mathrm{Z} \tag{24a}$$

$$s.t. \quad \text{(23b)} - \text{(23d)}, \text{(23f)} - \text{(23h)} \tag{24b}$$

Since $a_{uk}[n]$ is a binary decision variable. Problem **(P2)** is a mixed integer programming problem, it is difficult to solve it directly. However, we can define the variable return values as binary variables and solve them with the Moesk solver. The Moesk solver in CVX can solve mixed integer programming problems based on convex optimization algorithms and exhaustive search (such as branch and bound algorithms). Related applications of the solution can be found in the paper in Wang et al. (2020b)

4.2 Time slot allocation optimization

To optimize $\boldsymbol{t_u}$, $\boldsymbol{t_d}$ and $\boldsymbol{t_c}$ with fixed $\boldsymbol{A}$, $\boldsymbol{Q}$, and $\boldsymbol{P}$, the objective function and the associated constraints can be written as

(**P3**) :

$$\max_{t_u, t_d, t_c, \mathrm{Z}} \quad \mathrm{Z} \tag{25a}$$

$$s.t. \quad \text{(23b)} - \text{(23d)}, \text{(23i)} - \text{(23j)} \tag{25b}$$

It is observed that the objective function and the constraints (25a)–(25b) are linear, then we can solve **(P3)** by CVX.

4.3 UAVs' trajectory optimization

To optimize $\boldsymbol{Q}$ with fixed $\boldsymbol{t}_u$, $\boldsymbol{t}_d$, $\boldsymbol{t}_c$, $\boldsymbol{A}$ and $\boldsymbol{P}$, the objective function and the associated constraints can be written a

(**P4**) :

$$\max_{Q,Z} \quad Z \tag{26a}$$

$$s.t. \quad \text{(23b)} - \text{(23e)}, \text{(23k)} - \text{(23l)} \tag{26b}$$

Although the constraint (23k) is linear with respect to the variable $\boldsymbol{Q}$, the presence of the objective functions and constraints (23b)–(23d) and (23l) results in the problem remaining a complex nonconvex problem.

Since equations (23b)–(23d) contain multi-UAV trajectory variables that are coupled with each other, solving them directly is extremely challenging. Therefore, we adopted the BCD method to solve multi-UAV trajectories. We assigned an initial trajectory to each UAV, optimize the trajectory of one UAV while keeping the trajectories of other UAVs fixed, and update this UAV's trajectory. In this way, each UAV trajectory is optimized. The u-th UAV's optimization problem can be rewritten as follows.

(**P4.1**) :

$$\max_{Q_u,Z} \quad Z \tag{27a}$$

$$s.t. \quad \text{(23b)} - \text{(23e)}, \text{(23k)} - \text{(23l)} \tag{27b}$$

We noted that $\mathrm{R_k}$ is convex with respect to the variable $\| q_u[n] - w_k[n]\|^2$, which can be solved by successive convex optimization techniques. In each iteration, we used the Taylor series expansion of $\mathrm{R_k}$ to replace itself and obtain an approximate optimal solution. $\| q_u^{(l)}[n] - w_k[n]\|^2$ represents the Taylor series expansion points of the l-th iteration. $\mathrm{R_k}$ in each time slot can be replaced by its lower bound, defined as

$$\mathrm{R_k^{lb}} = \frac{1}{Nt} \sum_{u=1}^{U} \sum_{n=1}^{N} B a_{uk}[n] L_{uk}^{lb}[n] t_u[n] \tag{28}$$

To simplify the formula we replaced the constant $\| q_u^{(l)}[n] - w_k[n]\|^2$ in the Taylor expansion with ψ.

$$\begin{aligned} L_{uk}^{lb}[n] &= log_2\left(1 + \frac{F_{uk}^{(l)}[n]}{\psi} + H^2\right) \\ &\quad - C_{uk}^{lb}[n](\| q_u[n] - w_k[n]\|^2 - \psi) \\ &\le \log_2\left(1 + \frac{P_{uav} h_{uk}[n]}{\delta^2 + \sum_{j=1, j\neq u}^{U} P_{uav} h_{jk}[n]}\right) \end{aligned} \tag{29}$$

where

$$F_{uk}^{(l)}[n] = \frac{P_{uav}\beta_0}{\delta^2 + \sum_{j=1, j\neq u}^{U} P_{uav} h_{jk}[n]} \tag{30}$$

$$C_{uk}^{(l)}[n] = -\frac{log_2(e) F_{uk}^{(l)}[n]}{(H^2 + \psi)^2 + F_{uk}^{(l)}[n] H^2 + F_{uk}^{(l)}[n]\psi} \tag{31}$$

It is noted that $\| q_u[n] - w_k[n]\|^2$ is a convex function with respect to $q_u[n]$, so R^{lb} is also convex with respect to $q_u[n]$. Then constraint (23b) is transformed to convex constraint.

It is observed that $E_k[\mathrm{n}]$ is convex with respect to $\| q_u[n] - w_k[n]\|^2$, so $E_k[\mathrm{n}]$ can obtain its lower bound $E_k^{lb}[\mathrm{n}]$ by Taylor series expansion to obtain an approximate optimal solution

$$\begin{aligned} E_k^{lb}[n] &= \frac{\varepsilon a_{uk}[n] P_c[n] t_c[n] \beta_0}{H^2 + \psi} \\ &\quad - \left[\begin{array}{l} (\| q_u[n] - w_k\|^2 - \psi) \\ \times \frac{\log_2(e)\varepsilon a_{uk}[n] P_c[n] t_c[n] \beta_0}{(H^2+\psi)^2} \end{array}\right] \end{aligned} \tag{32}$$

$$E_k^{lb}[n] \ge a_{uk}[n] P_{iotd} t_u[n] \tag{33}$$

Then constraint (23c) is converted to convex constraint.

For the left-hand side of the constraint (23d) we can obtain its lower bound by Taylor series expansion, and for the right-hand side of the inequality we introduced a relaxation variable to obtain its upper bound. To simplify the formula we replaced the constant $\| q_u^{(l)}[n] - w_m[n]\|^2$ in the Taylor expansion with ρ, and we have

$$D_{au}^{lb}[n] \ge D_{uk}^{ub}[n] \; n \in \mathcal{N} \tag{34}$$

where

$$\begin{aligned} D_{au}^{lb}[n] &= B_u \log_2\left(1 + \frac{F_{au}^{(l)}[n]}{\rho + H^2}\right) \\ &\quad - C_{au}^{(l)}[n](\| q_u[n] - w_m[n]\|^2 - \rho) \\ &\le B_u \log_2\left(1 + \frac{P_u[n] h_{au}[n]}{\delta^2 + \sum_{j=u+1}^{U} P_j[n] h_{ju}[n]}\right) t_d[n] \\ &= D_{au}[n] \end{aligned} \tag{35}$$

$$\begin{aligned} D_{uk}^{ub}[n] &= a_{uk}[n] B_i \log_2\left(1 + \frac{P_{uav} \frac{\beta_0}{H^2 + \theta_{u,k}[n]}}{\delta^2 + \sum_{j=1, j\neq u}^{U} P_{uav} h_{jk}[n]}\right) t_u[n] \\ &\ge a_{uk}[n] B_i \log 2\left(1 + \frac{P_{uav} \frac{\beta_0}{H^2 + \| q_u[n] - w_k[n]\|^2}}{\delta^2 + \sum_{j=1, j\neq u}^{U} P_{uav} h_{jk}[n]}\right) t_u[n] \end{aligned}$$

$$= D_{uk}[n] \tag{36}$$

where, $\theta_{u,k}[n]$ is the slack variable we introduced to make the right-hand side of the constrained (23d) inequality convex obeys the following constraint.

$$\theta_{u,k}[n] \leq \| q_u^{(l)}[n] - w_k[n]\|^2 \ \forall u \in \mathcal{U}, k \in \mathcal{K}, n \in \mathcal{N} \tag{37}$$

Adopting slack variables does not cause the original problem to lose its optimal solution because the right-hand sides of (23d) and (36) are equivalent when (37) is set to the equal sign. If not, the value of $\theta_{u,k}[n]$ can be gradually decreased to obtain an upper bound for $D_{uk}^{ub}[n]$. The constraint (37) leads to a problem that is not yet a standard convex optimization problem. To address this, we converted (37) into a linear constraint by performing a Taylor series expansion.

$$\begin{aligned} &\| q_u^{(l)}[n] - w_k[n]\|^2 + 2(q_u^{(l)}[n] - w_k)(q_u[n] - w_k^{(l)}[n]) \\ &\geq \theta_{u,k}[n] n \in \mathcal{N}, u \in \mathcal{U}, k \in K \end{aligned} \tag{38}$$

As for (23l), it can be used continuous convex optimization techniques to transform it into a linear constraint.

$$\begin{aligned} &- \| q_u^{(l)}[n] - q_j[n]\|^2 + 2(q_u^{(l)}[n] - q_j^{(l)}[n])^T (q_u[n] - q_j[n]) \\ &\geq d_{\min}^2 n \in \mathcal{N}, u \in \mathcal{U}, j \in \mathcal{U}, j \neq u \end{aligned} \tag{39}$$

Through the above series of transformations. The original problem can be reformulated as

(**P4.2**) :

$$\max_{Q_u, \theta u, Z} \ \mathrm{Z} \tag{40a}$$

$$s.t. \ \ \mathrm{R_k^{lb}} \geq \mathrm{Z} \ \ \forall \mathrm{k} \in \mathcal{K} \tag{40b}$$

$$E_k^{lb} \geq E_0 \ \ \forall u \in \mathcal{U} \tag{40c}$$

$$D_{au}^{lb}[n] \geq D_{uk}^{ub}[n] \ \ n \in \mathcal{N} \tag{40d}$$

$$(23e), (23k) \tag{40e}$$

$$(38) - (40) \tag{40f}$$

It can be seen problem **(P4.2)** has been transformed into a standard convex optimization problem that can be solved by CVX.

4.4 AP's power distribution

To optimize $\boldsymbol{P}$ with fixed $\boldsymbol{t}_u$, $\boldsymbol{t}_d$, $\boldsymbol{t}_c$, $\boldsymbol{A}$ and $\boldsymbol{Q}$, the objective function and the associated constraints can be written as

(**P5**) :

$$\max_{P,Z} \ \mathrm{Z} \tag{41a}$$

$$s.t. \ \ (23d), (23m) - (23o) \tag{41b}$$

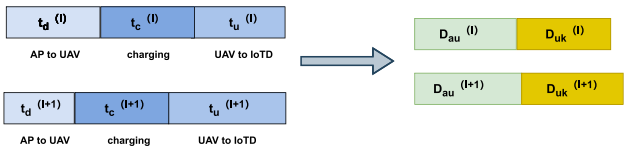

Fig. 3 Problem P5 conversion

The theoretical transmission rate sent by AP to the u-th UAV at the n-th time slot is calculated as

$$R_u[n] = B_u log_2 \left(1 + \frac{P_u[n]h_{au}[n]}{\delta^2 + \sum_{j=u+1}^{U} P_j[n]h_{aj}[n]}\right) \tag{42}$$

We can see that the transmission rate between AP and UAV is affected by the AP power allocation. So, we can improve its transmission rate by optimizing the power allocation, which will further effect the boundaries of constraints in (23d). Specifically, We can see from Fig. 3 that due to the increase of the rate from APs to UAVs, the time t_d spent on transmitting data decreases, which leads us to have more time t_u allocated for UAVs to forward the data to IoTDs. Therefore, D_{uk} will be improved further leading to the improvement of the objective function.

Since the objective function does not contain the variable $\boldsymbol{P}$, and in order to maximize the transmission rate from the AP to the UAV to allow the UAV have more time t_u to transmit data to the IoTDs, and thus to maximize the objective function $\boldsymbol{Z}$ in problem **(P5)**. We formulated the following problem concerning the maximization of the sum of the transmission rates from the AP to the UAV. The specific optimization objective and constraints can be written as

(**P5.1**) :

$$\max_{P[n]} \ \sum_{u=1}^{U} R_u[n] \ \ n \in \mathcal{N} \tag{43a}$$

$$s.t. \ \ (23d), (23m) - (23o) \tag{43b}$$

The object function and constraints (23d) are nonconvex. We firstly splited the expression in (23d) containing the variable $\boldsymbol{P}$ into the difference of two concave functions. The process is as follows

$$\begin{aligned} &\log_2 \left(1 + \frac{P_u[n]h_{au}[n]}{\delta^2 + \sum_{j=u+1}^{U} P_j[n]h_{aj}[n]}\right) \\ &= \log_2 \left(\delta^2 + \sum_{i=u}^{U} P_i[n]h_{ai}[n]\right) \end{aligned}$$

$$-\log_2\left(\delta^2+\sum_{j=u+1}^{U}P_j[n]h_{aj}[n]\right) \tag{44}$$

To further convert (44) to convex, we use SCA to replace the second half in (44) with its Taylor series expansion. The derivation process is as follows

$$\begin{aligned}G_{aj}^{lb}[n]&=\log_2\left(\delta^2+\sum_{j=u+1}^{U}P_j^{(l)}[n]h_{aj}[n]\right)\\&+(P_j[n]-P_j^{(l)}[n])\frac{\sum_{j=u+1}^{U}h_{aj}[n]}{\delta^2+\sum_{j=u+1}^{U}P_j^{(l)}[n]h_{aj}[n]}\\&\le\log_2\left(\delta^2+\sum_{j=u+1}^{U}P_j[n]h_{aj}[n]\right)\end{aligned} \tag{45}$$

Then we can obtain a lower bound on the transmission rate of the UAV.

$$R_u^{lb}[n]=B_u\left(\log_2\left(\delta^2+\sum_{i=u}^{U}P_i[n]h_{ai}[n]\right)-G_{aj}^{lb}[n]\right) \tag{46}$$

And problem **(P5.1)** is rewritten as

(**P5.2**) :

$$\max_{P[n]}\ \sum_{u=1}^{U}R_u^{lb}[n]\quad n\in\mathcal{N} \tag{47a}$$

$$s.t.\quad R_u^{lb}t_d[n]\ge D_{uk}[n]\quad n\in\mathcal{N} \tag{47b}$$

$$(23\text{m})-(23\text{o}) \tag{47c}$$

Since the problem **(P5.2)** is a convex problem, we can obtain an approximately optimal solution to the original problem by solving it with the CVX solver.

4.5 Overrall algorithm

In this section, we proposed an overall iterative algorithm, as shown in **Algorithm 1**. We optimized variables $\boldsymbol{A}$, $\boldsymbol{U}$, $\boldsymbol{t}_u$; $\boldsymbol{t}_d$; $\boldsymbol{t}_c$ and $\boldsymbol{P}$ by solving subproblems **(P2)**, **(P3)**, **(P4.2)** and **(P5.2)**. Among them, **(P4.2)** and **(P5.2)** are approximately optimal solutions due to the continuous convex approximation technique. Therefore what we get in **Algorithm 1** is an approximately optimal solution at least.

dummy

Algorithm 1 : Iterative Alternating Algorithm

1: **initialize** $A^{(0)}$, $t_u^{(0)}$,$t_d^{(0)}$, $t_c^{(0)}$, $Q^{(0)}$, $P^{(0)}$,l=0
2: **Repeat**
3: Solving problem **(P2)** by the given $t_u^{(l)}$, $t_d^{(l)}$, $t_c^{(l)}$, $Q^{(l)}$ and $P^{(l)}$, the obtained solutions can be expressed as $A^{(l+1)}$.
4: Solving problem **(P3)** by the given $A^{(l+1)}$, $Q^{(l)}$ and $P^{(l)}$, the obtained solutions can be expressed as $t_u^{(l+1)}$, $t_d^{(l+1)}$ and $t_c^{(l+1)}$.
5: **For** (u=1,u ≤ U,u++)
6: Solving problem **(P4.2)** by the given $A^{(l+1)}$, $t_u^{(l+1)}$, $t_d^{(l+1)}$, $t_c^{(l+1)}$,$P^{(l)}$, $Q_i^{(l)}$ $(i\in U, i\neq u)$ the obtained solutions can be expressed as $Q_u^{(l+1)}$.
7: **Update** $Q_u^{(l)}$
8: **End**
9: Solving problem **(P5.2)** by the given $A^{(l+1)}$, $t_u^{(l+1)}$, $t_d^{(l+1)}$, $t_c^{(l+1)}$ and $Q^{(l+1)}$, the obtained solutions can be expressed as $P^{(l+1)}$.
10: **Update** l=l+1.
11: **Until** Optimization variables converge within the given accuracy.

4.6 Complexity and convergence

4.6.1 Complexity analysis

Since the CVX solver is based on the interior point method, its complexity is $O(n^{3.5}\log(1/\varepsilon))$, where n represents the number of variables and ε represents the target accuracy. Therefore, the complexity of steps 3, 4, (5–7), and 8 are as follows

$$\begin{aligned}L1&=O((NK)^{3.5}\log(1/\varepsilon))\\L2&=O((3N)^{3.5}\log(1/\varepsilon))\\L3&=O((NU)^{3.5}\log(1/\varepsilon))\\L4&=O(N(U)^{3.5}\log(1/\varepsilon))\end{aligned}$$

The overall complexity of the final algorithm can be represented as $O(l\times(L1+L2+L3+L4))$. where l represents the total number of iterations of the algorithm.

4.6.2 Convergence analysis

The value of the objective function is defined as Z. To simplify the expression, we denote the three optimization variables t_u,t_d and t_c by T_s.

$$\begin{aligned}&Z(A^l,T_s^l,Q^l,P^l)\\&\overset{(a)}{\le}Z(A^{l+1},T_s^l,Q^l,P^l)\\&\overset{(b)}{\le}Z(A^{l+1},T_s^{l+1},Q^l,P^l)\\&\overset{(c)}{\le}Z(A^{l+1},T_s^{l+1},Q^{l+1},P^l)\\&\overset{(d)}{\le}Z(A^{l+1},T_s^{l+1},Q^{l+1},P^{l+1})\end{aligned} \tag{48}$$

Table 1 Parameters settings

Parameters	Value
Bandwidth B_u, B_i	40 MHz, 20 MHz
Length of each time slot t	0.1 s
Number of time slots N	300
Minimum task size $D_{\min}$	5×10^5 bit
Total transmit power of the AP P_{ap}	20 W
Transmitting power of UAV P_{uav}	1 W
receiving power of IoTD P_{iotd}	0.1 mw
Charging power of UAV P_c	47 dBm
Noise power δ^2	−40 dBm
Channel power gain β_0	−20 dB
Safe distance $d_{\min}$	10 m
Maximum flight speed $V_{\max}$	10 m/s
Energy conversion efficiency ε	0.85

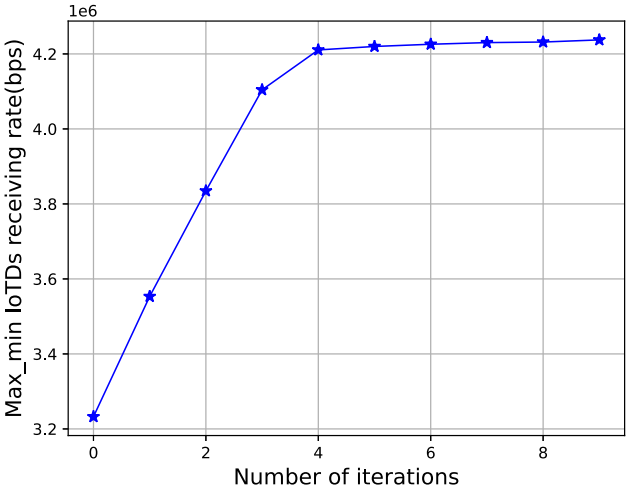

Fig. 4 The convergence of proposed algorithm

Firstly, we analyzed the iterative process in a round. Since all our subproblems **(P2)**, **(P3)**, **(P4.2)**, and **(P5.2)** already satisfy the standard convex problem. Therefore, during the l-th round, the solution of each subproblem leads to a gradual convergence of the objective function, which means that the inequalities (a), (b), (c) and (d) hold.

In order to analyze the convergence between the l-th and the (l+1)-th round, we further denote the optimized results for these two rounds as $Z^{(l)}$ and $Z^{(l+1)}$ respectively. Actually, the $Z^{(l)}$ equals to $Z(A^l, T_s^l, Q^l, P^l)$, and $Z^{(l+1)}$ equals to $Z(A^{l+1}, T_s^{l+1}, Q^{l+1}, P^{l+1})$ in (48). According to the inequalities (a), (b), (c) and (d), we know that $Z^{(l)} \leq Z^{(l+1)}$, which means the objective function Z converges between any two rounds. When the difference between any two objective values of adjacent rounds is less than a threshold, the algorithm completes convergence.

5 Numerical results

In this section, we conducted a comprehensive analysis of numerical results to verify the effectiveness of the algorithm. Our system consists of $M = 2$ UAVs, $K = 10$ IoTDs and an AP. we assumed that all UAVs fly at an altitude of $H = 5$ m and all IoTDs are randomly distributed in a horizontal area of 200 m × 200 m. For detailed parameter settings we referred to Wang et al. (2020b) and Xu et al. (2018), as shown in Table 1.

Firstly, Fig. 3 verifies the convergence of our algorithm. It can be seen that the objective function does not increase after several iterations. This indicates the high efficiency of our algorithm. Figure 5 provides a comparison between our optimized trajectory and the initial trajectory. By visualizing these trajectories, we can evaluate the effectiveness of our algorithm in improving the trajectory planning. It is worth noting that when designing the initial trajectory, several aspects need to be considered. Firstly, the initial trajectory should be as simple as possible and cover most IoTDs. Additionally, we need to ensure that the initial trajectory satisfies our collision prevention constraint. Therefore, the initial trajectories of UAV 1 and UAV 2 have the center coordinates (50, 100) and (140, 90) respectively, and the radius of the trajectory circle is set to 45 m. At the same time, we initialized the power allocation of the AP based on the initial trajectory. We initialized 12W and 8W to the UAVs with poor and good channel gain for each time slot, respectively. The optimized trajectory shows that the UAV will be as close as possible to the served IoTDs to obtain a higher channel gain, which will also increase the transmission rate. Figure 5 shows the comparison between the initial and optimized trajectories of the UAV, and it can be seen that UAVs trajectory is optimized to be closer to IoTDs, which is to get a better channel to improve the transmission rate.

Figure 6 shows a comparison of the average receiving rates of the different IoTDs in the initial and optimized trajectories. From Fig. 6, it is evident that optimizing the flight trajectory of the UAV results in a significant improvement in the transmission rate. The improvement of IoTD1, IoTD3, and IoTD9 is more noticeable. This is because they are further away from the initial trajectory.

Figure 7 illustrates the correlation between the speed of the UAV and the variation in time gap. From the data in the figure we can get that UAV 1 will reduce its speed when approaching the IoTD to get a better channel gain and then has traveled faster to the next IoTD.

To evaluate the performance of our algorithm, we optimized $\boldsymbol{P}$ and $\boldsymbol{A}$ by different methods, respectively. For AP power allocation, we firstly adopted two fixed allocation algorithms, one is to allocate to strong IoTD and weak IoTD

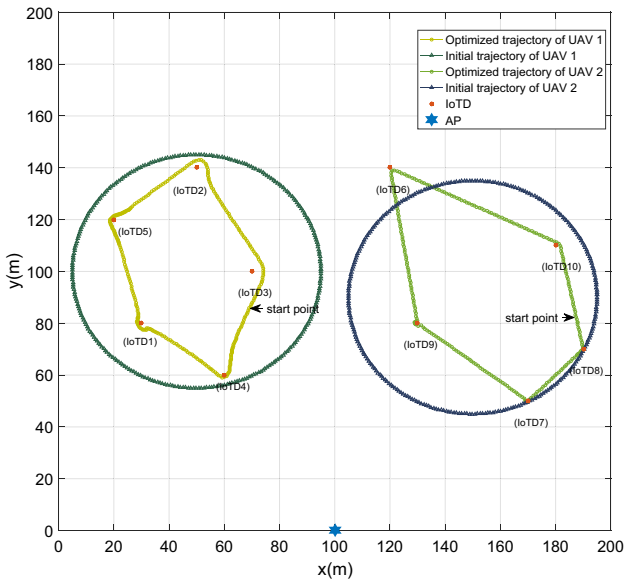

Fig. 5 Initial and optimized trajectory of UAVs

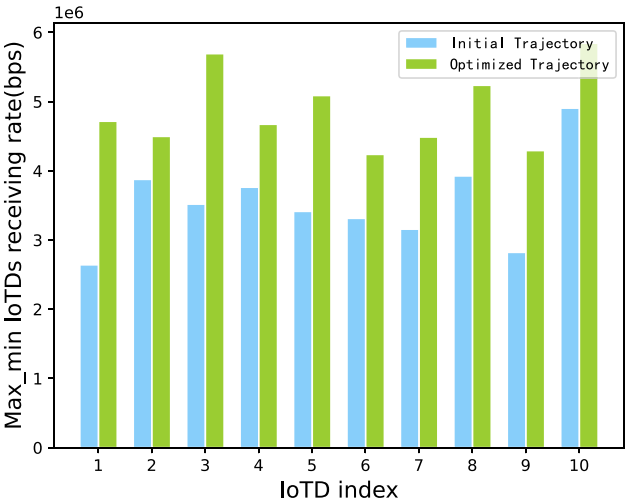

Fig. 6 IoTDs receiving rates for initial and optimized trajectories

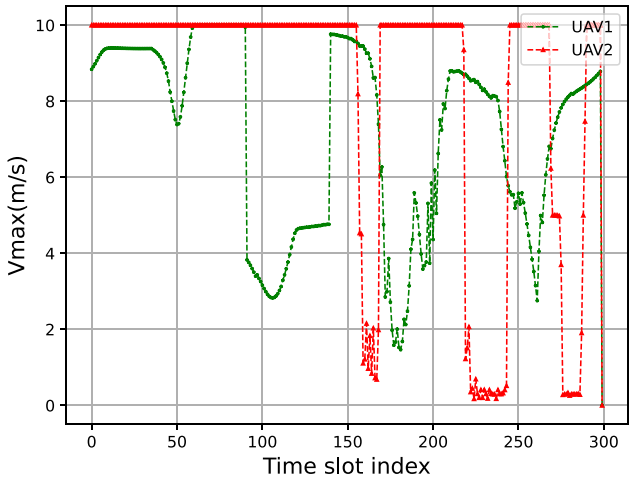

Fig. 7 UAVs flight speed

Table 2 Algorithm Runtime

IoTD numbers	Algorithm		
	FP	GS	ICOS
8	3078.2310 s	3313.3541 s	3109.3243 s
9	3189.4272 s	3578.1475 s	3220.2345 s
10	3312.7241 s	3710.2365 s	3355.6174 s
11	3457.3793 s	3896.8173 s	3489.7421 s
12	3589.6313 s	4063.5356 s	3616.4725 s

according to 20% and 80% of the total power. this allocation algorithm is defined as "FP1". The other allocation method is 40% and 60%, defined as "FP2". In addition, we used a global search method that lists all power allocations with an accuracy of 0.001W, following the NOMA power allocation principle, which is named 'GS' algorithm. Our algorithm is named the "ICOS" algorithm. Figure 8a, b show the variation of the objective function for different settings of the number of IoTDs and the total AP power, respectively. It can be observed that the objective function decreases as the number of users increases. This is because the number of time slots allocated to each user decreases in each cycle. In addition, increasing the total power of the AP will enhance the transmission rate from the AP to the UAV, thereby further improving the transmission rate from the UAV to the IoTDs.

The figure demonstrates that our algorithm surpasses the FP algorithm and is closed to the GS algorithm. However, the GS algorithm takes more time to sample, which we can see from Table 2 that the runtime of the GS algorithm is higher than that of ICOS. Figure 9 shows the power allocated to different UAVs by our power allocation algorithm at each time slot.

For the optimization of connection scheduling, our algorithm is compared with two other methods. One is a random connection(RC), in which the UAV selects a random IoTDs connection at each time slot, and the other is the closest connection(CC), where the UAV selects the closest IoTD to communicate with at each time slot. Figure 10a, b show the variation of the objective function for different settings of the maximum flight speed and the number of IoTDs, respectively. We can learn from the figure that the RC connection algorithm has the worst performance because of its stochastic nature. the CC algorithm is close to our performance, but since our optimization objective is to maximize the minimum average receiving rate of IoTDs, the CC algorithm may result in some of the IoTDs that are far away from the UAV with less number of connections not being able to obtain the optimal solution.

To verify the performance of NOMA and SIC technologies, we compared them with conventional OFDMA

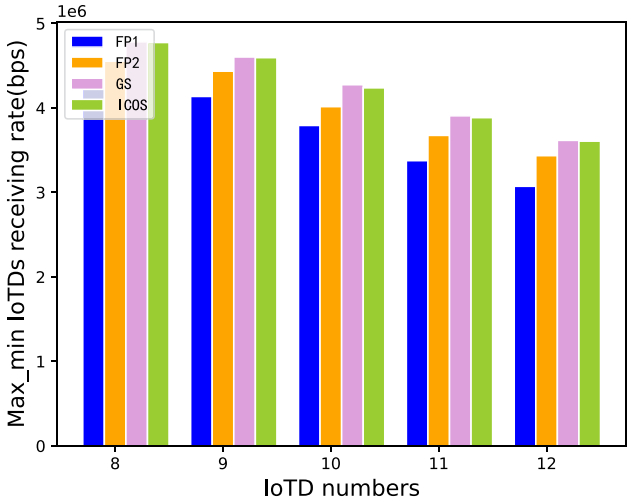

(a) IoTD numbers

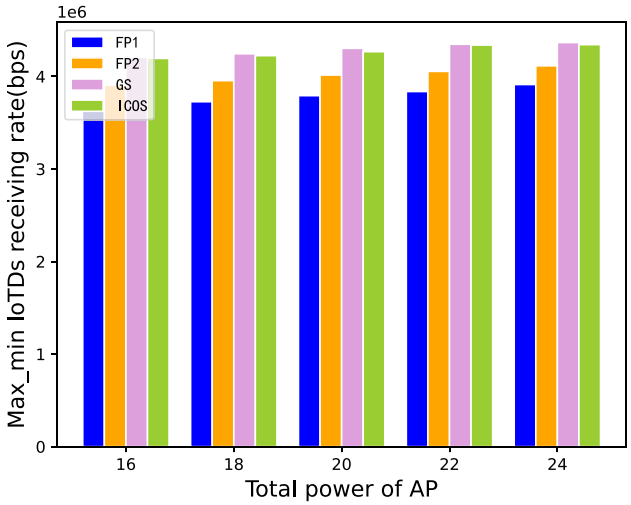

(b) Total power of AP

Fig. 8 Comparison of power distribution algorithms

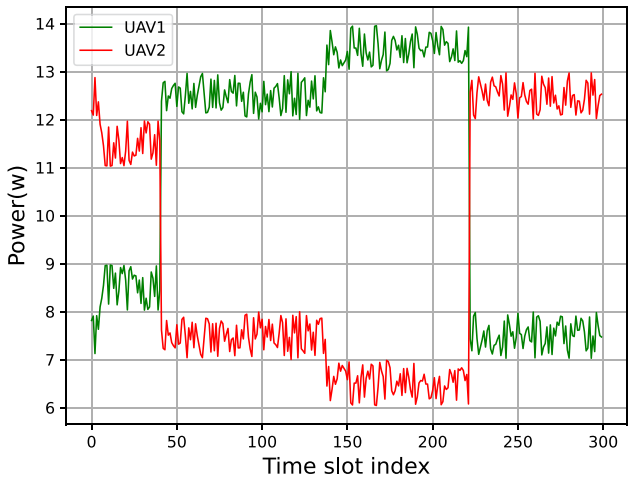

Fig. 9 Power Distribution

technologies. We splited the bandwidth and power equally to each UAV. Figure 11 compares the sum of the transmission rates of the UAVs at each time slot for OFDMA and NOMA. It can be seen that NOMA and SIC technologies have better transmission rates compared to traditional OFDMA.

Figure 12 shows the performance of the algorithm for different maximum flight speeds and total time **T**. It can be observed that as the maximum $V_{\max}$ increases, there is a slight increase in the objective function. This is because the UAV takes less time to fly from the previous IoTD to the next IoTD, resulting in a longer time around the IoTD to obtain a better channel to transmit data, which in turn improves the objective function. Also, it is clearly observed that as the total time increases, the optimization objective also increases. This is attributed to the fact that when the **T** is large enough, the percentage of UAV flight time will be small, and the UAVs will spend more time around IoTDs to get a more efficient transfer rate.

Figure 13 shows a comparison of the optimization objectives of the UAV at different flight altitudes and transmission power. From the figures, it can be seen that the objective function increases with increasing transmission power. This is because a higher transmission power results in a larger Signal to Interference plus Noise Ratio (SINR), which in turn leads to a higher transmission rate. In addition, as the UAV's altitude increases, the optimization objective decreases due to a decrease in channel gain and transmission rate.

6 Conclusion

In this paper, we proposed a relay system consisting of an AP and multiple UAVs. The AP is responsible for sending data to the UAVs, and the UAVs assist in forwarding data to the IoTDs and charging them to ensure proper data receiving. We set the optimization goal of maximizing the minimum receiving rate among all IoTDs and utilized NOMA and SIC techniques at the AP side to enhance the receiving rate. The system model is formulated as a nonlinear mixed-integer programming problem which can be further decomposed into subproblems by using the BCD method. For the nonconvex constraints in the subproblem, we used convex optimization methods such as successive convex approximation and relaxation variables and transform them into convex constraints to obtain an approximate optimal solution. Finally, we proposed an overall iterative algorithm. In the simulation results, we demonstrated the convergence of the algorithm and compared it with other benchmark algorithms. In addition, we also compared the effects of different parameters on our opti-

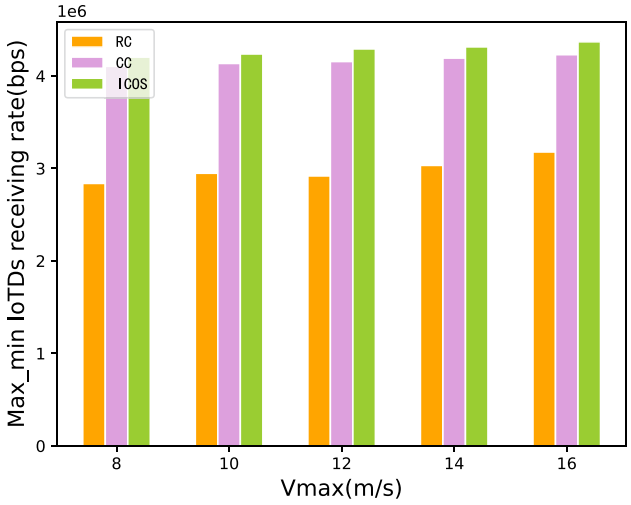

(a) Maximum flight speed

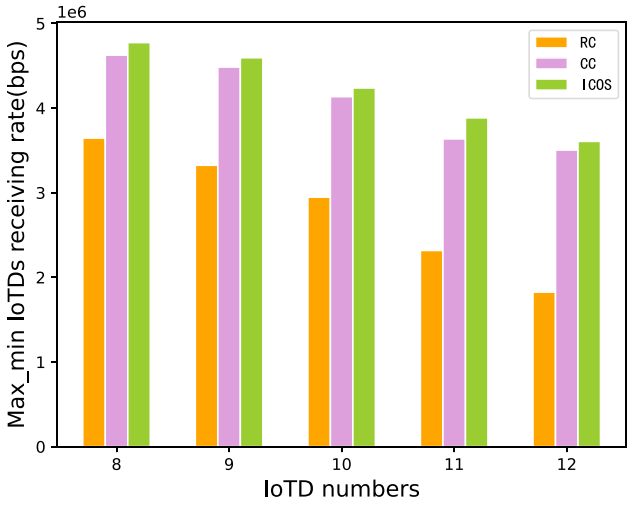

(b) IoTDs Numners

Fig. 10 Comparison of connection selection algorithms

mization objectives, such as the maximum flight speed of the UAV, the flight altitude and the number of IoTDs, etc. In future research work, we will further increase the number of UAVs to cope with huge number of IoTDs and use the reinforcement learning to address this large-scale MEC related problem.

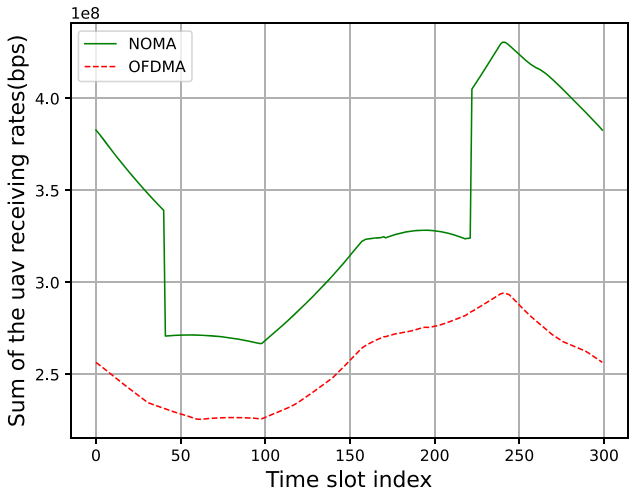

Fig. 11 Comparison of OFDMA and NOMA

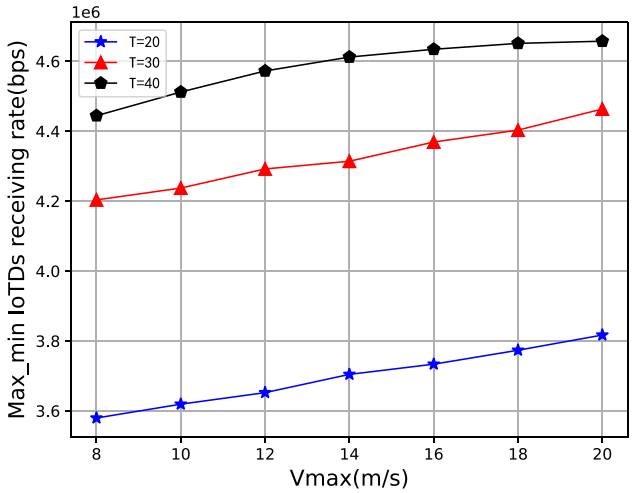

Fig. 12 Receiving rate VS maximum speeds and number of time slots

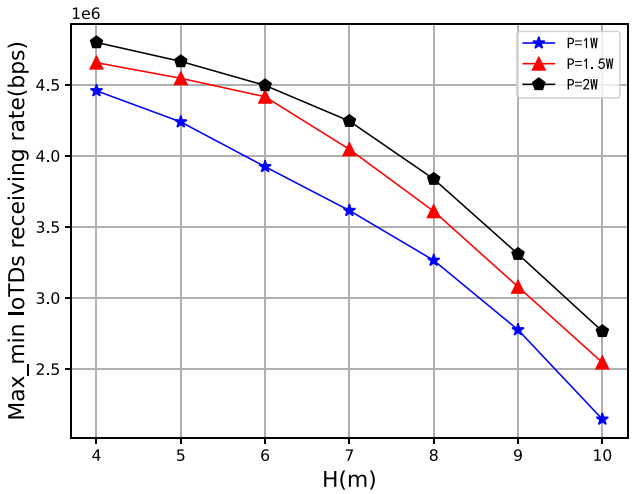

Fig. 13 Receiving rate VS transmission power and flight altitude

Author Contributions All authors contributed to the study conception and design. QT and XQ were responsible for model building, problem solving and the first draft of the paper. JW and SH advised on model building and checked the grammar and organization of the paper. All authors read and approved the final manuscript.

Funding This work is jointly supported by A Project Supported by Scientific Research Fund of Hunan Provincial Education Department (Grant No. 23A0258), Hunan Provincial Natural Science Foundation of China (Grant No. 2021JJ30736, 2023JJ50331), Changsha Municipal Natural Science Foundation (Grant No.kq2014112), Natural Science Foundation of China (Grant No. 62272063).

Data availability The datasets generated and analysed during the current study are available from the corresponding author on reasonable request.

Declarations

Conflict of interest We declare that we have no financial and personal relationships with other people or organizations that could unduly influence our research work, nor do we have any professional or other interests of any nature that could influence our position.

Ethical approval This article does not contain any studies with animals performed by any of the authors.

References

Baek H, Lim J (2019) Time mirroring based csma/ca for improving performance of uav-relay network system. IEEE Syst J 13(4):4478–4481

Diao X, Zheng J, Wu Y, Cai Y, Anpalagan A (2019) Joint trajectory design, task data, and computing resource allocations for noma-based and uav-assisted mobile edge computing. IEEE Access 7:117448–117459

Gao H, Zhang S, Su Y, Diao M, Jo M (2019) Joint multiple relay selection and time slot allocation algorithm for the eh-abled cognitive multi-user relay networks. IEEE Access 7:111993–112007

Islam SR, Avazov N, Dobre OA, Kwak K-S (2016) Power-domain non-orthogonal multiple access (noma) in 5g systems: potentials and challenges. IEEE Commun Surv Tutor 19(2):721–742

Ji Y et al (2020) Multicell edge coverage enhancement using mobile uav-relay. IEEE Internet Things J 7(8):7482–7494

Jiang X, Wu Z, Yin Z, Yang W, Yang Z (2019) Trajectory and communication design for uav-relayed wireless networks. IEEE Wirel Commun Lett 8(6):1600–1603

Jing Y, Jafarkhani H (2009) Single and multiple relay selection schemes and their achievable diversity orders. IEEE Trans Wirel Commun 8(3):1414–1423

Katwe M, Singh K, Sharma PK, Li C-P, Ding Z (2021) Dynamic user clustering and optimal power allocation in uav-assisted full-duplex hybrid noma system. IEEE Trans Wirel Commun 21(4):2573–2590

Kim SH, Chaitanya TV, Le-Ngoc T, Kim J (2015) Rate maximization based power allocation and relay selection with iri consideration for two-path af relaying. IEEE Trans Wirel Commun 14(11):6012–6027

Li B, Fei Z, Zhang Y (2019) Uav communications for 5g and beyond: recent advances and future trends. IEEE Internet Things J 6(2):2241–2263

Liu X et al (2023) Ris-uav enabled worst-case downlink secrecy rate maximization for mobile vehicles. IEEE Trans Veh Technol 72(5):6129–6141

Liu G, Wang Z, Hu J, Ding Z, Fan P (2019) Cooperative noma broadcasting/multicasting for low-latency and high-reliability 5g cellular v2x communications. IEEE Internet Things J 6(5):7828–7838

Liu B, Wan Y, Zhou F, Wu Q, Hu RQ (2022) Resource allocation and trajectory design for miso uav-assisted mec networks. IEEE Trans Veh Technol

Mirbolouk S, Valizadeh M, Amirani MC, Ali S (2022) Relay selection and power allocation for energy efficiency maximization in hybrid satellite-uav networks with comp-noma transmission. IEEE Transa Veh Technol 71(5):5087–5100

Miridakis NI, Vergados DD (2012) A survey on the successive interference cancellation performance for single-antenna and multiple-antenna ofdm systems. IEEE Commun Surv Tutor 15(1):312–335

Rezvani S, Jorswieck EA, Joda R, Yanikomeroglu H (2022) Optimal power allocation in downlink multicarrier noma systems: theory and fast algorithms. IEEE J Select Areas Commun 40(4):1162–1189

Seid AM et al (2021) Collaborative computation offloading and resource allocation in multi-uav-assisted iot networks: A deep reinforcement learning approach. IEEE Internet Things J 8(15):12203–12218

Wang H et al (2018a) Power control in uav-supported ultra dense networks: communications, caching, and energy transfer. IEEE Commun Mag 56(6):28–34

Wang H et al (2018b) Power control in uav-supported ultra dense networks: communications, caching, and energy transfer. IEEE Commun Mag 56(6):28–34

Wang B et al (2020a) Graph-based file dispatching protocol with d2d-enhanced uav-noma communications in large-scale networks. IEEE Internet Things J 7(9):8615–8630

Wang J, Na Z, Liu X (2020b) Collaborative design of multi-uav trajectory and resource scheduling for 6g-enabled internet of things. IEEE Internet Things J 8(20):15096–15106

Xu J, Zeng Y, Zhang R (2018) Uav-enabled wireless power transfer: trajectory design and energy optimization. IEEE Trans Wirel Sommun 17(8):5092–5106

Yadav A, Quan C, Varshney PK, Poor HV (2020) On performance comparison of multi-antenna hd-noma, scma, and pd-noma schemes. IEEE Wirel Commun Lett 10(4):715–719

You C, Zhang R (2020) Hybrid offline-online design for uav-enabled data harvesting in probabilistic los channels. IEEE Trans Wirel Commun 19(6):3753–3768

Zeng J et al (2018) Investigation on evolving single-carrier noma into multi-carrier noma in 5g. IEEE Access 6:48268–48288

Zeng Y, Zhang R, Lim TJ (2016) Throughput maximization for uav-enabled mobile relaying systems. IEEE Trans Commun 64(12):4983–4996

Zhang G et al (2022) Cooperative uav enabled relaying systems: joint trajectory and transmit power optimization. IEEE Trans Green Commun Netw 6(1):543–557

Zhong X, Guo Y, Li N, Li S (2019) Deployment optimization of uav relays for collecting data from sensors: a potential game approach. IEEE Access 7:182962–182973